Spatial Modelling of the Temporal Patterns and Intensity of Wire Snare Poaching and Predicting Land Cover Change Dynamics in a Semi-Arid Protected Area

Article *in* African Journal of Ecology · April 2025

DOI: 10.1111/aje.70040

3 authors:

Nobert Tafadzwa Mukomberanwa
Chinhoyi University of Technology
17 PUBLICATIONS **20** CITATIONS
SEE PROFILE

Patmore Ngorima
Zimbabwe Parks and Wildlife Management Authority
15 PUBLICATIONS **39** CITATIONS
SEE PROFILE

Thomas Musora
Chinhoyi University of Technology
8 PUBLICATIONS **6** CITATIONS
SEE PROFILE

African Journal of Ecology

WILEY

African Journal of Ecology

RESEARCH ARTICLE

Spatial Modelling of the Temporal Patterns and Intensity of Wire Snare Poaching and Predicting Land Cover Change Dynamics in a Semi-Arid Protected Area

Nobert Tafadzwa Mukomberanwa[1] | Patmore Ngorima[2] | Thomas Musora[3]

[1]Department of Geoinformatics and Environmental Conservation, Chinhoyi University of Technology, Chinhoyi, Zimbabwe | [2]Zimbabwe Parks and Wildlife Management Authority, Scientific Services Unit-Marongora Field Station, Karoi, Zimbabwe | [3]Department of Mathematics and Statistics, Chinhoyi University of Technology, Chinhoyi, Zimbabwe

Correspondence: Nobert Tafadzwa Mukomberanwa (nobertmukomberanwa@gmail.com)

Received: 19 November 2024 | **Revised:** 24 March 2025 | **Accepted:** 26 March 2025

Keywords: autoregressive integrated moving average | cellular automata artificial neural network | kernel density | time series forecasting | wire snare poaching

ABSTRACT

The spatial and temporal dynamics of poaching, along with continuous land cover alterations like deforestation and agricultural expansion, hinder efficient wildlife management. Changes in land cover could either generate new poaching opportunities or impede access to previously exploited areas. With the doubling of Africa's human population, protein resources will be strained, boosting the purchase and harvest of bushmeat for sustenance and income. In regions where meat poaching transpires, wire snaring is a prevalent technique due to its affordability, efficacy, and ease of acquisition, installation, and concealment. Due to their non-selective nature, snares can inflict severe by-catch mortality on a range of species. Yet, the necessity of projecting future values of a time series traverses across a range of fields. Powerful methods have been developed to capture these components by defining and estimating statistical models. Policymakers must plan several months or years ahead, since drawing up policies and actual policy implementation may take several months or years. The aims of this study were to (i) estimate the spatiotemporal patterns and intensity of wire snare poaching and (ii) predict future land cover dynamics using land change models and assess how these changes may influence poaching risk in the coming years. The Autoregressive Integrated Moving Average (ARIMA) was utilised for time series analysis and forecasting. Kernel density estimator (KDE) was used to smooth point data (in this case the locations of wire snares) to create a continuous surface that shows areas of high and low density. The analysis of land use and land cover takes into account the utilisation of Landsat satellite image products. Satellite images for the years 2020, 2022, and 2024 were utilised as inputs for forecasting future land cover scenarios using cellular automata artificial neural network (CA-ANN). The results from the ARIMA show an increase in the wire snares which would enhance the possibility for human–wildlife conflicts by the year 2028. Kernel density estimators pinpoint regions where wire snares are most concentrated; conservation teams can focus their patrols, thus helping to conserve species more efficiently. CA-ANN reveals marginal changes in land use and land cover which might enhance the likelihood for human–wildlife conflicts. Time series forecasting helps estimate when and where poaching activity is likely to spike. By identifying monthly trends, conservation teams can take preventative efforts rather than reacting after poaching has occurred.

1 | Introduction

Increasing demand for wild meat and wildlife products drives unsustainable levels of illegal hunting, including wire snares (Martin et al. 2020; Loveridge et al. 2020, Battisti 2024) also in the Mid Zambezi savannah biomes. Habitat loss and hunting are currently the twin threats to wildlife across the world (Eniang et al. 2017). As such, changes in land use and land cover (LULC) can influence the prevalence of wire snare poaching incidents by affecting wildlife habitat, increasing human access to formerly remote areas, and shifting human-wildlife interactions (Banerjee et al. 2020). The fragmentation of habitats, deforestation, agricultural expansion, infrastructure development, and other land use changes can all create conditions that make wildlife more vulnerable to poaching, including wire snaring (Djagoun and Gaubert 2009). As natural areas shrink, wildlife may increasingly come into contact with human settlements, farming areas, and roads (Wato et al. 2006). Poachers often exploit these interactions to set snares in accessible locations where animals are more likely to wander (Watson et al. 2013).

The Charara Safari Area, located in the ecologically diverse Mid-Zambezi Region, is experiencing rapid environmental changes due to anthropogenic pressures such as agricultural expansion and poaching. This study focuses on spatial modelling to understand the temporal patterns and intensity of wire snare poaching while predicting land cover change dynamics. Buffalo (*Syncerus caffer*), kudu (*Tragelaphus strepsiceros*), impala (*Aepyceros melampus*), and warthog (*Phacochoerus africanus*) populations are particularly affected by these threats, as they rely on the region's grasslands, forests, and water resources for survival. The interplay between habitat fragmentation, wildlife movements, and human activities highlights the need for comprehensive conservation strategies to address the ecological and socioeconomic challenges in the area (Watson et al. 2013). In areas with fewer prey species, poachers may still target certain species by setting snares in places where animals are likely to travel in search of food or water (Martin et al. 2020, Becker et al. 2024). With better access to forests, wildlife reserves, and protected areas, poachers can more easily set wire snares, particularly in regions where enforcement is weak or where there is a lack of surveillance (Martin et al. 2020; Loveridge et al. 2020). Understanding these links is essential for developing strategies to mitigate poaching and promote sustainable land-use practices that protect wildlife and their habitats (Loveridge et al. 2020). The dynamics of land cover change—whether due to natural or anthropogenic factors—can have cascading effects on poaching patterns, creating feedback loops that exacerbate both environmental degradation and poaching intensity. Understanding the spatiotemporal patterns of wire snare poaching and predicting land cover change dynamics in the Charara Safari Area is critical for effective conservation management. The ability to model these patterns and predict future trends will enable the development of more adaptive and proactive conservation strategies (Diebold and Rudebusch 2011). For instance, identifying hotspots of poaching activity over time can help prioritise patrolling and enforcement efforts (Moore et al. 2018), while forecasting land cover changes can inform land use planning and policy decisions (Mukomberanwa et al. 2024) aimed at reducing poaching pressures.

The final report on large predator camera trap surveys in the Zambezi Valley, Zimbabwe, recorded some worrying results on the number of wire snares (snare wound, scar, or wire) detected in the Mid-Zambezi Valley Region (Loveridge et al. 2020). The distribution of snared predators detected in the surveys highlighted the threat of bush-meat snaring in the western and eastern parts of the Zambezi Valley landscape (Loveridge et al. 2020). Results from the snare wounds and a Getis Ordis hotspot analysis suggested that more snaring pressure based on observations of lions (*Panthera leo*) and spotted hyenas (*Crocuta crocuta*) was observed in Charara Safari Area and Rifa, western portions of Nyakasanga, and eastern portions of Dande when compared with other protected areas in the Mid-Zambezi Valley Region (Loveridge et al. 2020). The analysis of snaring hotspots suggested that lion and spotted hyena detections occurred in the southern part of Charara Safari Area and the eastern part of Dande. These areas are also closest to human settlement and the main arterial roads and are most likely to be affected by bushmeat snaring. It is not possible to determine the exact origin of the snares as the predators detected with snares are likely to range widely and are not necessarily detected at or close to the point at which they were originally trapped. Overall, the population density of lions in the Zambezi Valley was relatively robust at 2.7 lions/100 km^2 and an estimated population of 333 adults and sub-adults. This is comparable to other similar ecosystems in the region. It is likely that if human pressures (human-wildlife conflict and bushmeat snaring) were alleviated on the periphery of the system, lion populations could increase in the Zambezi Valley system (Loveridge et al. 2020). Settlement on protected area edges can often lead to increases in human-wildlife conflict and there are frequent reports of conflicts with large predators over livestock depredation in the farming areas around the protected area complex (Madden 2004). The impact of this is not known, though losses of wild animals to retaliatory killing and problem animal control seem likely (Fentaw and Duba 2017). Therefore, this study aims to (i) model the spatiotemporal patterns and intensity of wire snare poaching using time series methods and (ii) predict future land cover dynamics using land change models and assess how these changes may influence poaching risk in the coming years in the Charara Safari Area, Mid Zambezi region. We hypothesise that (i) the spatial and temporal distribution of wire snare poaching in the Charara Safari Area is influenced by proximity to water sources, roads, and human settlements, with increased poaching intensity occurring during the dry season and therefore (ii) areas with high poaching activity correlate with significant changes in land cover, indicating that poaching pressure contributes to land degradation and habitat alteration over time.

2 | Materials and Methods

2.1 | Study Area

The study was conducted in Charara Safari Area in north western Zimbabwe, with Zambia to their north, covering an area of 1692 km^2 (Figure 1). Charara is part of the Lower Zambezi Valley, with Lake Kariba and the Zambezi River being an important part of its ecosystem, and it is also part of the KAZA landscape. The area comprises a low-lying floodplain along the shores of Lake Kariba, with a mountainous interior (Chakuya

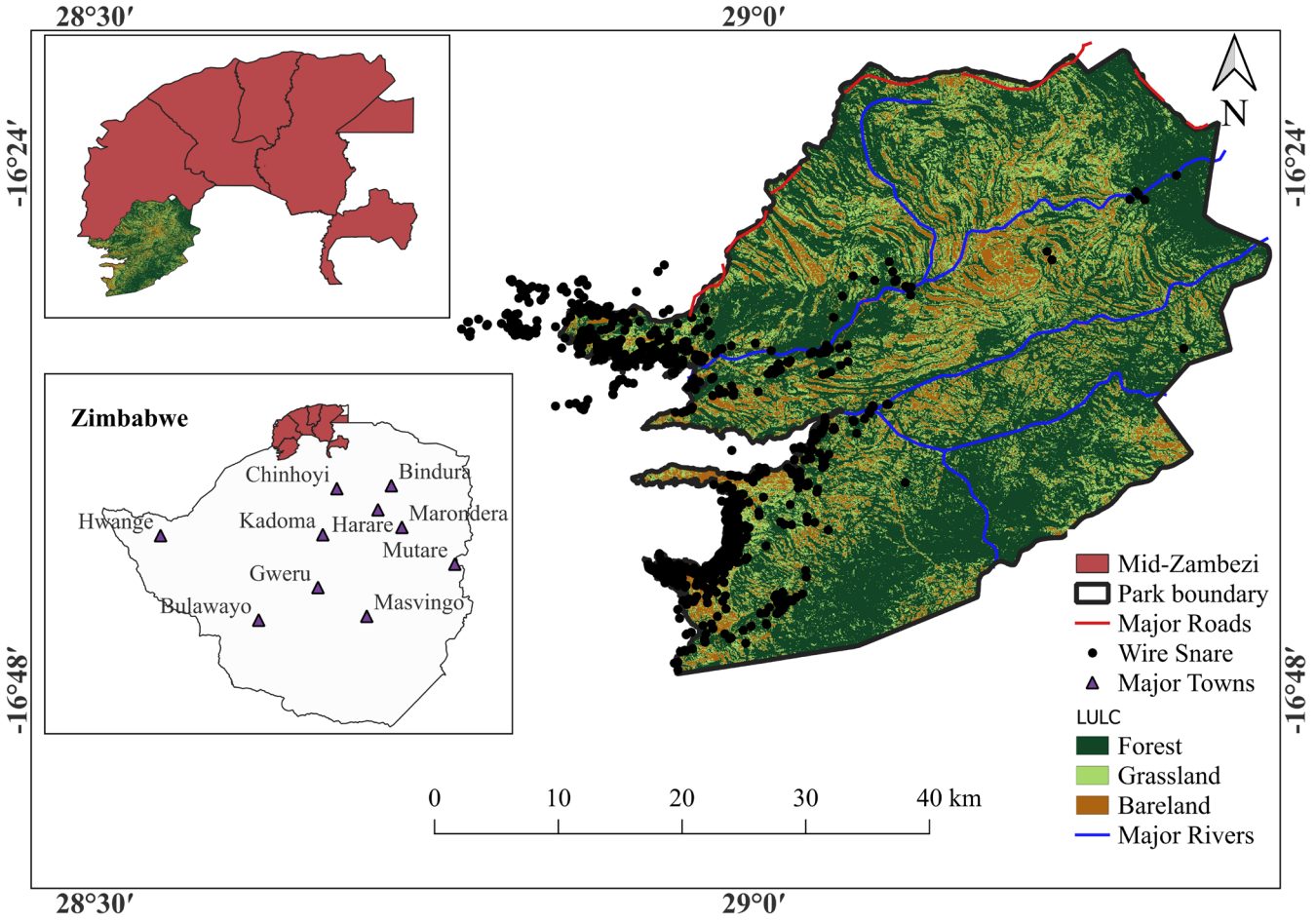

FIGURE 1 | Location of Charara Safari Area with land use and land cover (LULC) classes (Forest, grassland, and bareland). The Charara Safari Area is located within the Mid-Zambezi region.

et al. 2023). Rainfall occurs from November to April, and annual rainfall varies between 400 and 800 mm (Dunham et al. 2015). The region is generally hot and dry, with an average mean temperature of 31°C, with minimum temperatures of 26°C recorded in July and a maximum of 43°C recorded in October (Dunham et al. 2015). Charara is a state-owned hunting safari area, with several fishing and safari camps under the management of Zimparks (Dunham et al. 2015). It is surrounded by several communal areas such as Kanyati, Nyaodza, and Vuti on the eastern side, while its western boundaries lie on the shores of Lake Kariba, which makes it susceptible to the problem of snaring.

2.2 | Data Collection and Processing

The GPS location data of recovered wire snares used for this study were collected from August 2020 to July 2024. The data were collected at Marongora Field Station by the Zimbabwe Parks and Wildlife Management Authority (ZIMPARKS). The data were entered into an Excel sheet and statistical investigations for time series were done using Minitab and R-statistical programming respectively (R Development Core Team 2022). Land cover change dynamics were performed using cellular automata artificial neural network (CA-ANN) in Python programming. Maps layouts were created using ArcGIS Pro 3.0.

2.3 | Time Series Analysis and Modelling Strategy

2.3.1 | ARIMA Model

The ARIMA model is an extension of the ARMA model in the sense that by including auto-regression and moving average, it has an extra function for differencing the time series. If a dataset exhibits long-term fluctuations such as trends, seasonality, and cyclic components, differencing a dataset in ARIMA allows the model to deal with them. Two common processes of ARIMA for recognising trends in time-series data and forecasting are auto-regression and moving averages.

2.3.2 | Autoregressive Process

Most time series consist of elements that are serially dependent in the sense that one may estimate a coefficient or a collection of coefficients that describe subsequent elements of the series from specific, time-lagged (prior) elements. Each observation of

the time series is made up of random error components (random shock; (a_t) and a linear mixture of past observations).

2.3.3 | Moving Average Process

Independent from the autoregressive process, each element in the series might also be affected by past errors (or random shock) that cannot be accounted for by the autoregressive component. Each observation of the time series is made up of a random error component (random shock, ε) and a linear combination of earlier random shocks.

2.3.4 | Autoregressive Integrated Moving Average Process, ARIMA(p, d, q)

A series X_t is called an autoregressive integrated moving average process of orders p, d, q (where p is the order of the autoregressive component, d is the degree of differencing, and q is the order of the moving average component), ARIMA(p, d, q) if $W_i = \nabla^d X_t$, where W_i is the differenced time series.

We may define the difference operator ∇ as $\nabla X_t = X_t - X_{t-1}$. Differencing a time series $\{X_t\}$ of length n produces a new time series $\{W_t\} = \{\nabla^d X_t\}$ of length $n - d$.

If $\{Z_t\}$ is a purely random process with mean zero and variance σ_t^2, the general autoregressive integrated moving average process is of the form

$$W_t = \phi_1 W_{t-1} + \phi_2 W_{t-2} + \ldots + \phi_p W_{t-p} + Z_t + \theta_1 Z_{t-1} + \ldots + \theta_q Z_{t-q}$$

In terms of the backward shift operator, the ARIMA (p, d, q) process is F

$$\Phi_p(B)\, W_t = \Theta_q(B)\, Z_t$$

Remark. The autoregressive integrated moving average process is specifically for non-stationary time series. The differencing transformation is useful in reducing a non-stationary time series to a stationary one.

2.3.5 | Seasonal Autoregressive Integrated Moving Average Process

$$\text{ARIMA}(p, d, q)(P, D, Q)$$

Let s be the number of observations per season. Then the time series, X_t, is called a seasonal autoregressive integrated moving average process of orders p, d, q, seasonal orders P, D, Q and seasonal period s, if it satisfies;

$$\phi_p(B)\Phi_p(B)^s \nabla^d \nabla_s^D X_t = \theta_q(B)\Theta_Q(B^s) Z_t$$

where, $\nabla_s^D X_t = \sum_{j=0}^{D} \binom{D}{J} X_{i-js}$ and, $\phi_p(B)$ and $\theta_q(B)$ are polynomials in B of order p and q, that is;

$$\phi_p(B) = \left(1 - \theta_1 B_1 - \theta_2 B^2 - \ldots - \theta_p B^p\right)$$

$$\theta_q(B) = \left(1 - \phi_1 B_1 - \phi_2 B^2 - \ldots - \phi_q B^q\right)$$

We identified the stationary component of a data set by performing the Ljung and Box test. We tested this hypothesis by choosing a level of significance for the model adequacy and compared the computed Chi-square (χ^2) values with the (χ^2) values obtained from the table. If the calculated value is less than the actual (χ^2) value, then the model is adequate; otherwise not. The $Q(r)$ statistic is calculated by the following formula:

$$Q_{(r)} = n(n+2) \sum \frac{r^2(j)}{n-j}$$

where n is the number of observations in the series and $r(j)$ is the estimated correlation at lag j. Furthermore, we tested the data to identify the order of the regular and seasonal autoregressive and moving average polynomials necessary to effectively reflect the time series model. For this reason, model parameters were calculated using a maximum likelihood technique that reduced the sums of squared residuals and maximised the likelihood (probability) of the observed series. The maximum likelihood estimation is often the favoured least squares technique. The key tools utilised in the identification phase are plots of the series, correlograms (plots of autocorrelation and partial autocorrelation versus lag) of the autocorrelation function (ACF) and the partial autocorrelation function (PACF). The ACF and the PACF are the most important parts of time series analysis and forecasting. The ACF assesses the amount of linear dependency between observations in a time series that are separated by a lag k. The PACF plot helps to identify how many autoregressive terms are necessary to display one or more of the following characteristics: time lags where large correlations arise, seasonality of the series, and trend either in the mean level or in the variance of the series. In diagnostic checking, the residuals from the fitted model were evaluated against their adequacy. This is commonly done by correlation analysis through the residual ACF plots and by goodness-of-fit tests utilising means of χ^2 statistics. At the forecasting stage, the estimated parameters were utilised to construct new values of the time series with associated confidence ranges for the forecasted values.

2.3.6 | Performance Evaluation

To identify the best model from the class of plausible models, the estimated parameters were tested for their validity using ACF, PACF, probability plots, and histogram of residuals, a time series plot of observed and fitted values, and other error statistics such as coefficient of determination (R^2) were analysed.

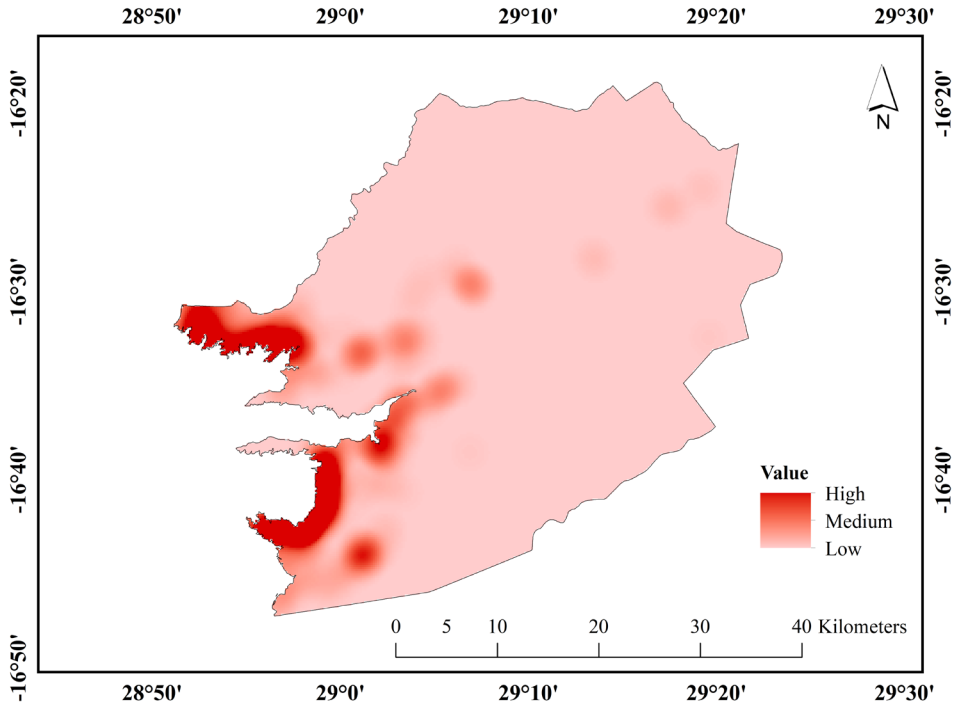

FIGURE 2 | Kernel density of wire snares in Charara Safari Area showing high and low density areas.

2.4 | Kernel Density Estimator for Wire Snares Data

The Kernel Density Estimator (KDE) is a vital spatial analysis tool for mapping and understanding the ecological impact of threats like poaching (Figure 2). It creates a smooth surface highlighting areas of high and low snare density, helping conservationists identify poaching hotspots in ecosystems such as the Charara Safari Area. KDE estimates the probability density function of point data—such as snare locations—over a geographic area. The process involves collecting GPS coordinates of detected snares, overlaying a grid, and applying a kernel function, typically Gaussian, which assigns weights to surrounding areas based on distance. Closer points receive higher weights, refining density estimates. Snare densities are classified into high, medium, and low, with patterns influenced by environmental and anthropogenic factors. The bandwidth parameter regulates KDE's sensitivity, balancing local detail with broader trends. A smaller bandwidth captures fine-scale poaching patterns, while a larger bandwidth smooths fluctuations. By integrating KDE with ecological variables like proximity to water sources, game trails, and human access points, conservationists can better understand poaching dynamics. The resulting heatmap guides anti-poaching patrols and resource allocation while enabling temporal analysis of poaching trends. This spatial approach strengthens conservation strategies, mitigating threats to wildlife and preserving ecosystem integrity.

2.5 | Prediction of Land Use Land Cover Change Using CA-ANN

Landsat 8 satellite imagery from 2020, 2022, and 2024 was analysed using Google Earth Engine (GEE) to assess land use and land cover (LULC) changes in the Charara Safari Area (Appendix 1). Supervised classification, employing a maximum likelihood classifier, was used to categorise images into forest, water, grassland, and bare land. Ground truthing verified the classification accuracy. The Classification and Regression Trees (CART) classifier was used due to its ability to handle complex environmental variables and partition data into subsets based on decision trees. The user guide of Climate Change Initiatives product gives accuracy ratings of the CCI-LC map year 2018 using the GlobCover 2009 validation dataset (Mukomberanwa et al. 2024). Overall accuracies turned out to be 82.45% employing "certain" whether "homogeneous" or "heterogeneous" points; what's more 76.4% was identified utilising only "homogeneous" and "certain" locations. Following classification, the area of each LULC class was computed using pixel area calculations, enabling quantification of ecological shifts over time. The study also projected future LULC changes for 2028 using Cellular Automata–Artificial Neural Networks (CA-ANN). This modelling approach, validated in prior studies (Mukomberanwa et al. 2024), integrates classified maps from 2020, 2022, and 2024 with spatial variables such as Digital Elevation Models (DEM) and slope (Appendix 2). DEMs, representing the Earth's topography, provide critical insights into landscape features that influence vegetation distribution, hydrological patterns, and erosion processes. Slope, an essential ecological factor, affects soil stability, water flow, and species composition, making it vital for predicting land cover transitions. A change detection analysis for 2020–2022 identified transitions between land cover classes, offering insight into deforestation, grassland expansion, and water body fluctuations (Appendix 3). The 2024 simulated map, generated from the model, was compared with actual 2024 satellite data to validate predictive accuracy (Appendix 4). This comparison

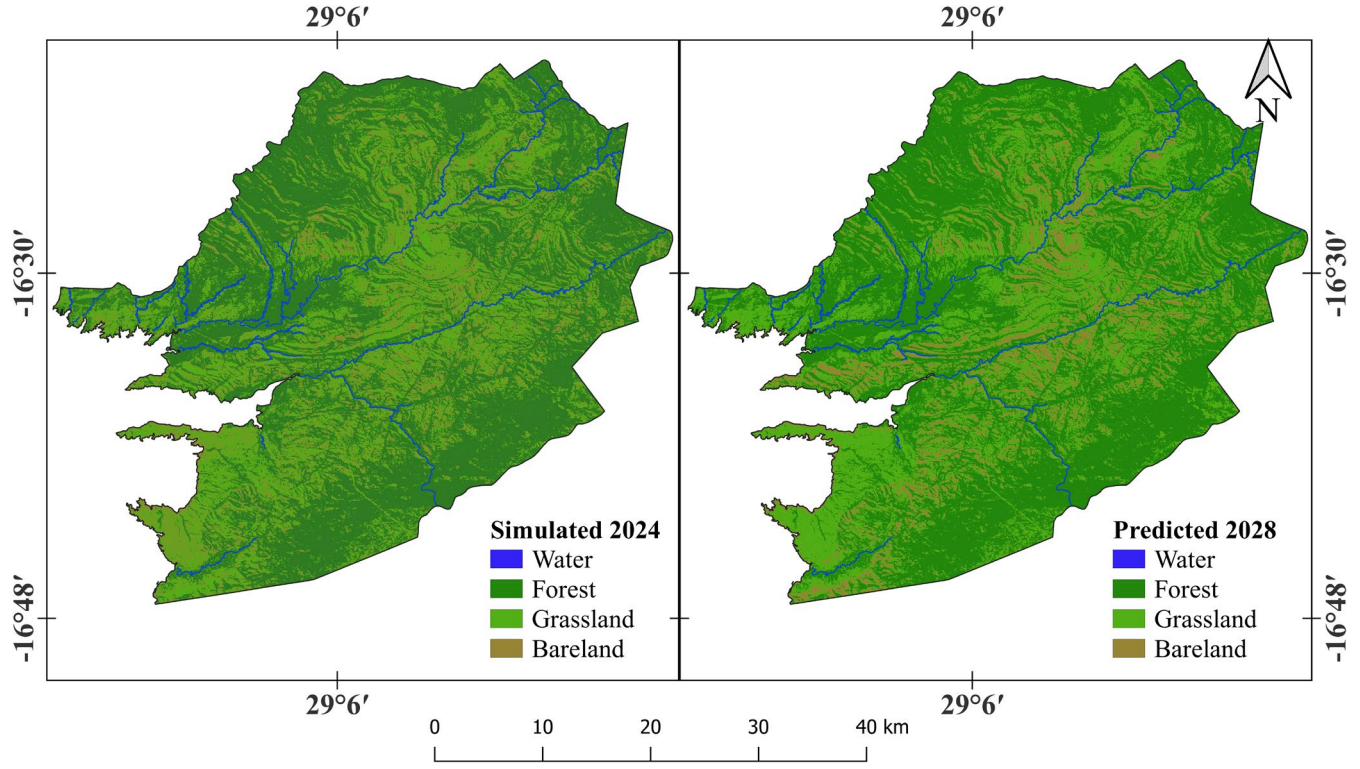

FIGURE 3 | Simulated and predicted landscape of the Charara Safari Area for the years 2024 and 2028, respectively.

ensured that the model correctly captured ecological dynamics before being applied to 2028 projections (Figure 3). In CA modelling, calibration and validation are crucial. The actual 2024 map (Appendix 1), derived from real-world observations, served as a benchmark to assess the reliability of the simulated 2024 map (Figure 3). By comparing these datasets, adjustments were made to improve model accuracy. Metrics such as overall accuracy and Kappa coefficient assessed the degree of agreement between the predicted and observed maps. A well-calibrated model provides a realistic basis for forecasting landscape transformations driven by factors like climate variability, human activities, and conservation policies.

3 | Results

3.1 | Time Series Analysis and Modelling Strategy

In our analysis, we show the following MINITAB simulation charts: A visual evaluation of Figure 4a,b and the augmented Dickey-Fuller test (original data) Tables 1 and 2 demonstrates that the series is stationary, and so a model may be fitted to this data. The Augmented Dickey-Fuller (ADF) test assesses the stationarity of the wire snare data to determine its suitability for ARIMA modelling. In the original data test, the test statistic of −6.15421 is significantly lower than the critical value of −2.92534 at a 0.05 significance level, with a p-value of 0.000 (Tables 1 and 2). This leads to rejecting the null hypothesis, indicating that the data is stationary and does not require differencing. Similarly, for the differenced data, the test statistic of −5.83473 is below the critical value of −2.94354, also rejecting the null hypothesis. This confirms the data remains stationary without further differencing (Tables 1a,b and 2). Thus, we can proceed to fit a model to this data. The ACF figure, Figure 5a, indicates no major spikes; the ACFs are practically nil, so a seasonal IMA model is advised. The PACF plot, Figure 5c, indicates a substantial spike at lag 7 with some indication of exponential decay; hence, this suggests there may be a need to further convert the data to be able to construct a more parsimonious model. The ACF plot, Figure 5b, indicates a considerable increase at lag 1, with the remainder of the ACFs basically nil, so a seasonal IMA model is suggested. The PACF plot, Figure 5d, indicates a substantial spike at lag 1 with some evidence of exponential decay; consequently, a seasonal IMA model is also suggested.

3.1.1 | Model Fitting

See Table 2.

3.1.2 | Model Diagnostics

Figure 6a displays no notable spikes, suggesting that there might be no conceivable extra factors that may have been neglected in this model. The PACF of residuals, Figure 6b, resists any noteworthy spikes, suggesting that there might be no conceivable extra parameters that may have been neglected in this model. Since the fitted model appears good enough, it can be utilised for projecting the future number of snares. Figure 6c indicates that no model assumption has been violated. Figure 6d is the actual forecast of snares for the year 2028.

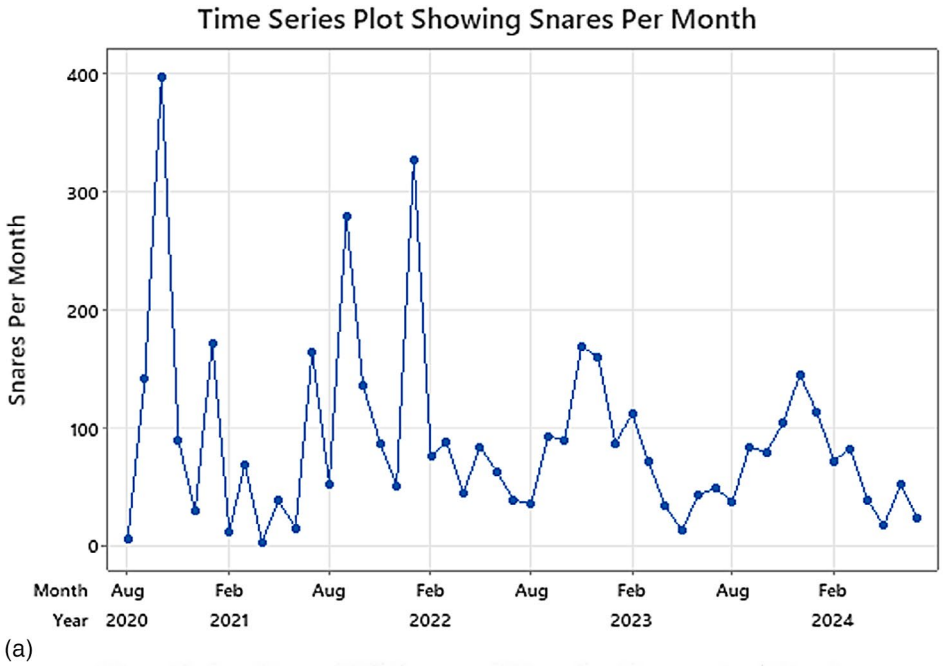

(a)

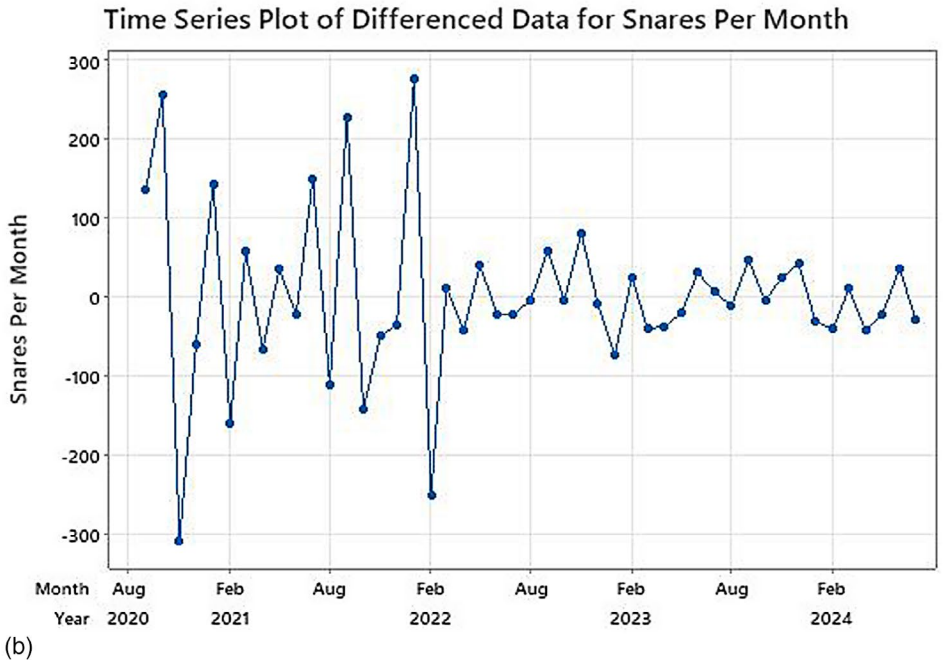

(b)

FIGURE 4 | (a) Time series plot for the original data, (b) time series plot for the differenced data.

3.2 | Kernel Density Estimator for Wire Snares Data

The Kernel Density Estimator (KDE) map illustrates the distribution of wire snares in the Charara Safari Area (Figure 2). The density is represented using a gradient of red shades, with darker red indicating high-density areas and lighter shades indicating lower densities. High-density regions, mainly concentrated along the western and southwestern parts of the study area, contain the highest number of snares per square kilometre. These areas likely exceed 5 snares per square kilometre. Medium-density regions, shown in intermediate red shades, likely have between 2 and 5 snares per square kilometre, while low-density areas, covering most of the study region, have fewer than 2 snares per square kilometre. Areas with high density or a higher number of snares are close to Lake Kariba and also near Kariba town. Areas with low density or a lesser number of snares are farther away from the town and the lake. Areas close to the lake experience a large number of snares since they are close to human settlements and, as such, poachers target areas close to water since they understand that the daily movement patterns of wildlife are driven by water.

3.3 | Prediction of Land Use Land Cover Change Using CA-ANN

The Charara Safari Area has experienced notable changes in land use and land cover over recent years, reflecting the impacts of human activities such as wildlife poaching using wire snares

TABLE 1 | (a) Augmented Dickey-Fuller test of original data and (b) augmented Dickey-Fuller test of differenced data.

Null hypothesis		**Data are non-stationary**
Alternative hypothesis		**Data are stationary**
Test statistic	***p***	**Recommendation**
(a) Augmented Dickey-Fuller test (original data)		
−6.15421	0.000	Test statistic ≤ critical value of −2.92534
		Significance level = 0.05
		Reject null hypothesis
		Data appears to be stationary, not supporting differencing
(b) Augmented Dickey-Fuller test (differenced data)		
−5.83473	0.000	Test statistic ≤ critical value of −2.94354
		Significance level = 0.05
		Reject null hypothesis
		Data appears to be stationary, not supporting differencing

TABLE 2 | Final estimates of parameters.

Type	**Coef**	**SE Coef**	***T***	***p***
MA 1	1.0356	0.0650	15.94	0.000
Constant	−1.759	0.883	−1.99	0.052

and agricultural encroachment. An analysis of data from 2020 to 2024 (Table 3), along with projections for 2028 (Figure 3), reveals significant shifts in the landscape. The water bodies within the region have remained relatively stable, with a slight increase from 51 km^2 in 2020 to 52 km^2 in 2024 (Table 3). This trend is expected to continue, with predictions indicating a minor increase to 52.5 km^2 by 2028. In contrast, the forest cover shows fluctuating patterns. The forested area expanded from 1223 km^2 in 2020 to a peak of 1313 km^2 in 2022, likely due to reforestation efforts or natural regrowth. However, it then decreased to 1176 km^2 by 2024, potentially due to increased agricultural encroachment and the impact of poaching on forest-dependent wildlife. Simulations and predictions suggest a partial recovery, with forest cover expected to rise to 1250 km^2 in 2024 and further to 1290 km^2 by 2028, possibly reflecting improved conservation measures. Grasslands have also undergone significant changes. The area covered by grasslands decreased sharply from 321 km^2 in 2020 to 270 km^2 in 2022 but rebounded to 325 km^2 by 2024. However, projections indicate a decline to 282 km^2 by 2028. The most dramatic change is observed in bareland, which initially decreased from 97 km^2 in 2020 to 58 km^2 in 2022, possibly due to vegetation recovery. However, by 2024, bareland increased to 139 km^2, indicating soil degradation, deforestation, or clearing for agriculture. Predictions suggest a reduction to 67.5 km^2 by 2028, which could reflect efforts to restore degraded lands. Overall, the total land area of 1692 km^2 has remained constant, indicating that the changes are shifts in land cover types rather than an expansion or contraction of the total area. A Root Mean Square Error (RMSE) value of 0.2 was obtained from the Neural Network learning curve (Figure 7) showing that the model can relatively predict the data accurately.

4 | Discussion

4.1 | Time Series Analysis and Modelling Strategy

This study demonstrates how ARIMA time series is beneficial to examine the prevalence of snares in the Charara Safari Area in the mid-Zambezi region in Zimbabwe. The ARIMA (0, 1, 1) forecasted the data significantly well and generated solid projections. According to the data presented, this model was best in forecasting the occurrence of snares but could not determine why the snare data had certain outliers. The time series forecasting system helped develop a model, the ARIMA time series model, that is effective for forecasting and can be applied to other conservatives predicting the predicted number of snares. However, it would be fascinating to perform further research on the factors that impact human-wildlife interactions, such as competing for key resources like water and food. This would consolidate better the nation's policy planning and policy implementation.

4.2 | Kernel Density Estimator for Wire Snares Data

The kernel density estimator (KDE) map of wire snare distribution in the Charara Safari Area provides critical ecological insights into the impact of poaching on wildlife. Covering 1692 km^2, the study area exhibits varying snare densities, with high-density regions predominantly in the western and southwestern sections. The dark red areas indicate concentrated snaring activity, likely due to favourable conditions for poachers, such as proximity to water sources, dense vegetation, and accessibility. The concentration of snares near water bodies and access routes suggests targeted poaching zones, requiring intensified conservation and anti-poaching measures. Understanding these density variations helps inform wildlife protection efforts and resource allocation for effective intervention strategies. Medium- and low-density areas, represented by lighter red shades, suggest scattered or infrequent snaring activities, potentially influenced by terrain, law enforcement presence, or lower wildlife densities. From an ecological perspective, high snare densities pose a significant threat to biodiversity, particularly for large herbivores and carnivores, which are primary targets for bushmeat and illegal wildlife trade. Species such as impalas, zebras, and buffaloes are especially vulnerable, as snares are indiscriminate, leading to severe injuries, slow deaths, and long-term population declines. Apex predators, including lions and leopards, also suffer from secondary impacts, as they may become caught in snares themselves or experience reduced prey availability due to increased poaching pressure.

The spatial distribution of snares indicates key ecological interactions. Areas with high snare densities often overlap with critical wildlife habitats, including feeding and breeding grounds. These

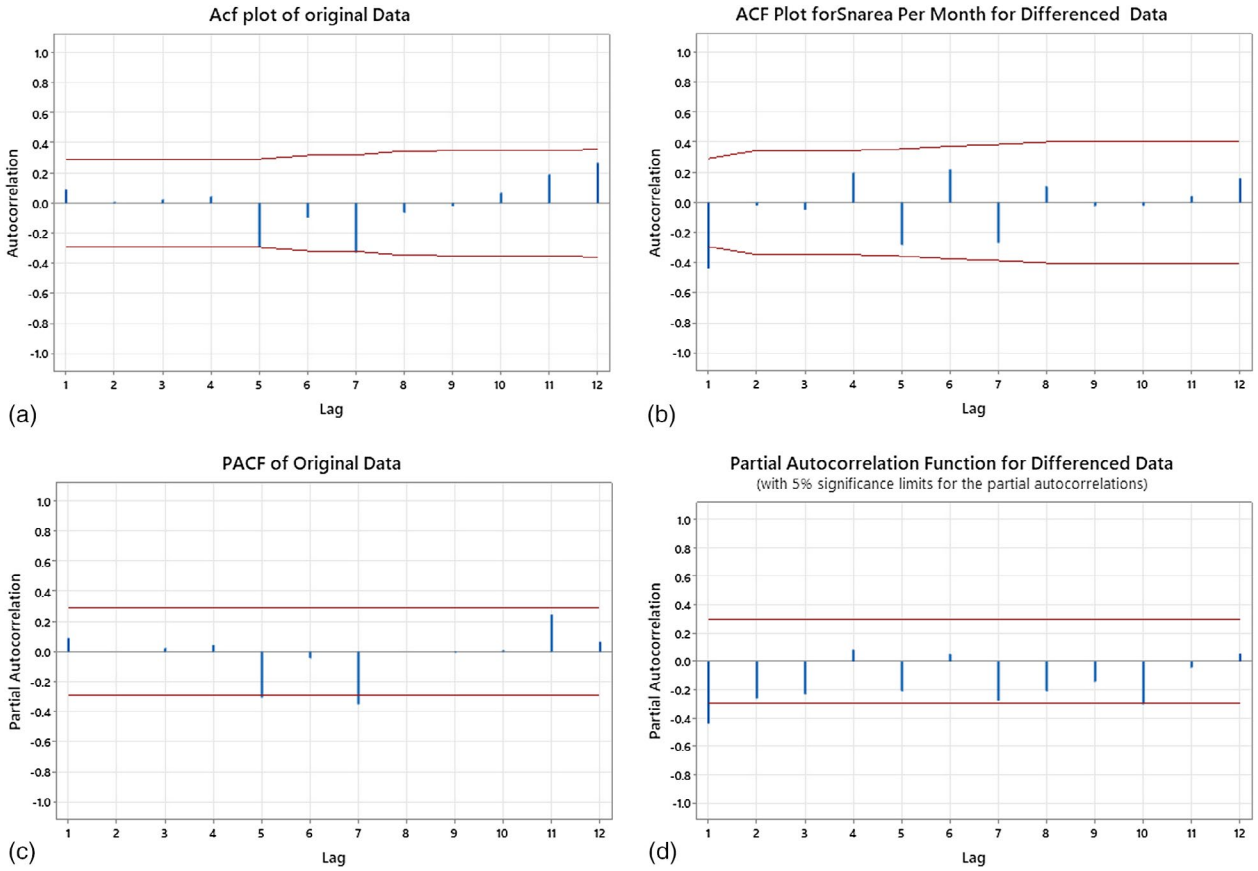

FIGURE 5 | (a) The autocorrelation function (ACF) plot of original data, (b) the autocorrelation function (AFC) plot of differenced data, (c) the partial autocorrelation function (PACF) of the differenced data, and (d) the partial autocorrelation function (PACF) plot of differenced data.

zones may coincide with seasonal migration routes, where animals move in predictable patterns, making them easy targets. This disrupts natural movement patterns, forcing animals to alter their behaviour to avoid heavily poached zones, which can lead to habitat fragmentation and increased human-wildlife conflicts.

The presence of medium and low snare density areas does not necessarily indicate safe zones for wildlife. Instead, it may reflect law enforcement patrol effectiveness, variations in vegetation cover, or differences in poacher activity. In areas where anti-poaching measures are stricter, snare densities may be lower due to increased risk for poachers. However, these areas remain at risk if enforcement weakens or if poachers adapt their strategies, shifting their activities to less monitored zones. The long-term ecological consequences of snaring in the Charara Safari Area extend beyond immediate wildlife mortality. A decline in herbivore populations can lead to cascading effects on vegetation dynamics, as reduced grazing pressure may alter plant community structures. Predators that rely on large prey species may experience population declines, leading to imbalances in trophic interactions. Additionally, the removal of key species from the ecosystem can trigger unintended ecological shifts, affecting biodiversity and ecosystem stability. Mitigation strategies should focus on increasing anti-poaching patrols in high-risk areas, enhancing community involvement in conservation, and employing technology such as camera traps and drones for real-time monitoring. Education and awareness programs can help reduce poaching by addressing underlying socio-economic drivers, such as food insecurity and unemployment. Ultimately, a multi-faceted approach combining law enforcement, ecological monitoring, and community engagement is necessary to curb snaring and preserve the ecological integrity of the Charara Safari Area.

4.3 | Prediction of Land Use Land Cover Change Using CA-ANN

The Charara Safari Area has experienced substantial changes in land use and land cover between 2020 and 2024, with projections extending to 2028. The analysis of classified images of land use and land cover (LULC) changes for the Charara Safari Area between 2020 and 2028 reveals significant shifts in the landscape, driven primarily by agricultural expansion and other human activities. These changes have profound ecological implications, particularly for the temporal patterns and intensity of wire snare poaching, which predominantly affect buffalo, impala, kudu, and warthog populations. The interaction between land use changes and poaching dynamics underscores the urgency of addressing both environmental and socioeconomic factors influencing the region.

The area covered by water remained relatively stable, increasing slightly by 2028. This stability suggests that water resources are currently less affected by human activities, although any future disruptions could alter this balance. Forest cover saw an increase

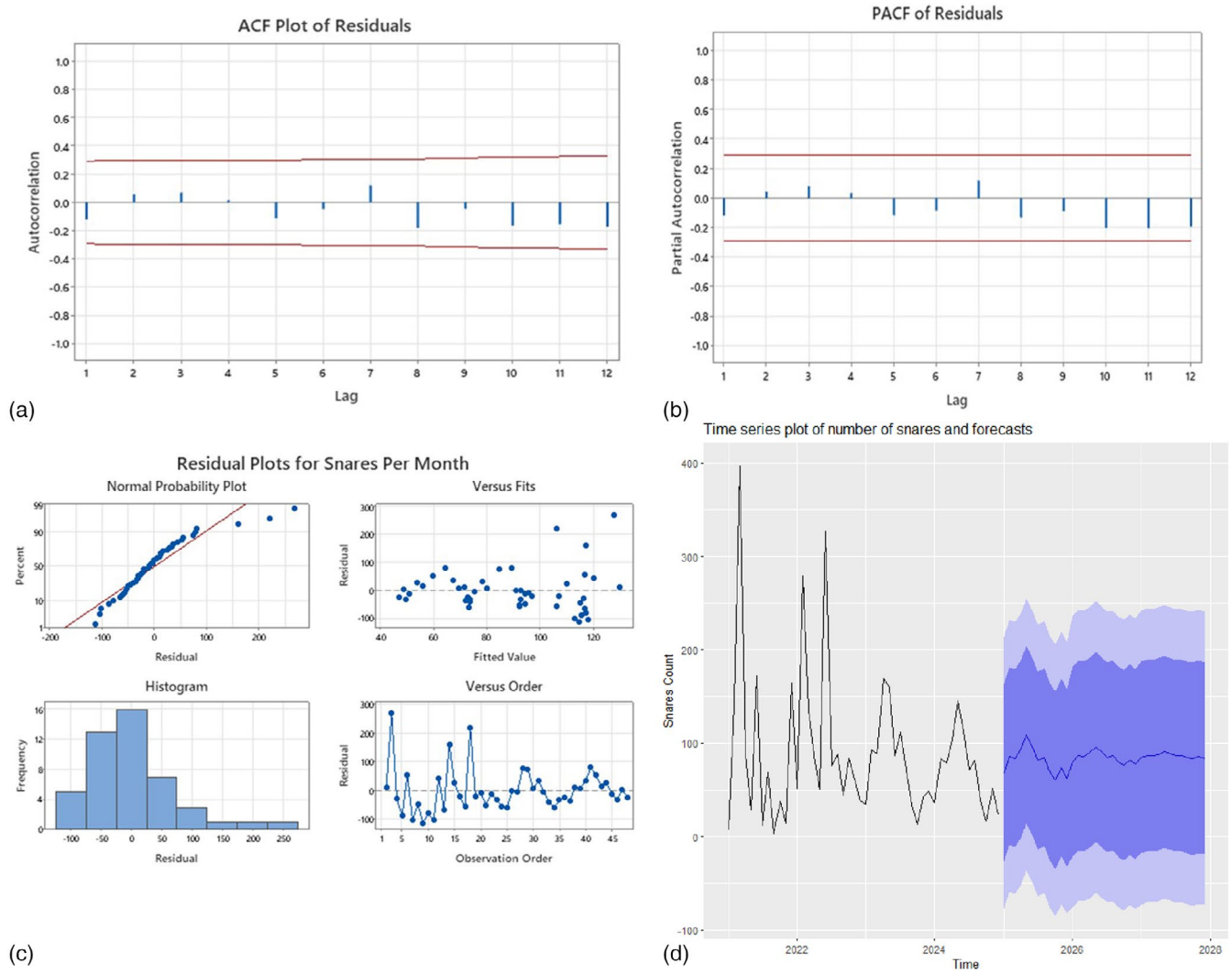

FIGURE 6 | (a) ACF plot of residuals, (b) PACF plot of residuals, (c) residual plots for snares per month, and (d) time series plot on number of snares and forecasts.

TABLE 3 | Land use and land cover data from 2020 to predicted 2028.

	2020	2022	2024	Simulated 2024	Predicted 2028
Water, km^2	51	51	52	51.2	52.5
Forest, km^2	1223	1313	1176	1250	1290
Grassland, km^2	321	270	325	310	282
Bareland, km^2	97	58	139	80.8	67.5
Total, km^2	1692	1692	1692	1692	1692

followed by a decline. Simulations suggest a recovery and a predicted expansion by 2028. Grassland cover decreased in 2022, before rebounding in 2024. However, a simulated decline and a further decrease by 2028 reflect ongoing pressures. This fluctuation could be attributed to habitat degradation from poaching activities and conversion to agricultural land, which disrupts the natural grassland ecosystem. This is a result of human encroachment into the Safari area since it is bordered by human settlements such as Kanyati, Nyaodza, and Vuti on the eastern side, while its western boundaries lie on the shores of Lake Kariba. Bare land decreased, then increased sharply in 2024. Simulations suggest it will decline again in 2028. These patterns highlight the urgent need for targeted conservation strategies to address poaching, agricultural encroachment, and land degradation to ensure the sustainability of the Charara Safari Area's diverse ecosystems. These changes highlight the dynamic nature of land use in the region, driven by both natural processes and human activities, such as agricultural expansion into the park's boundaries. While some recovery in forest and water areas is predicted, the ongoing pressure on grassland and bare land areas raises

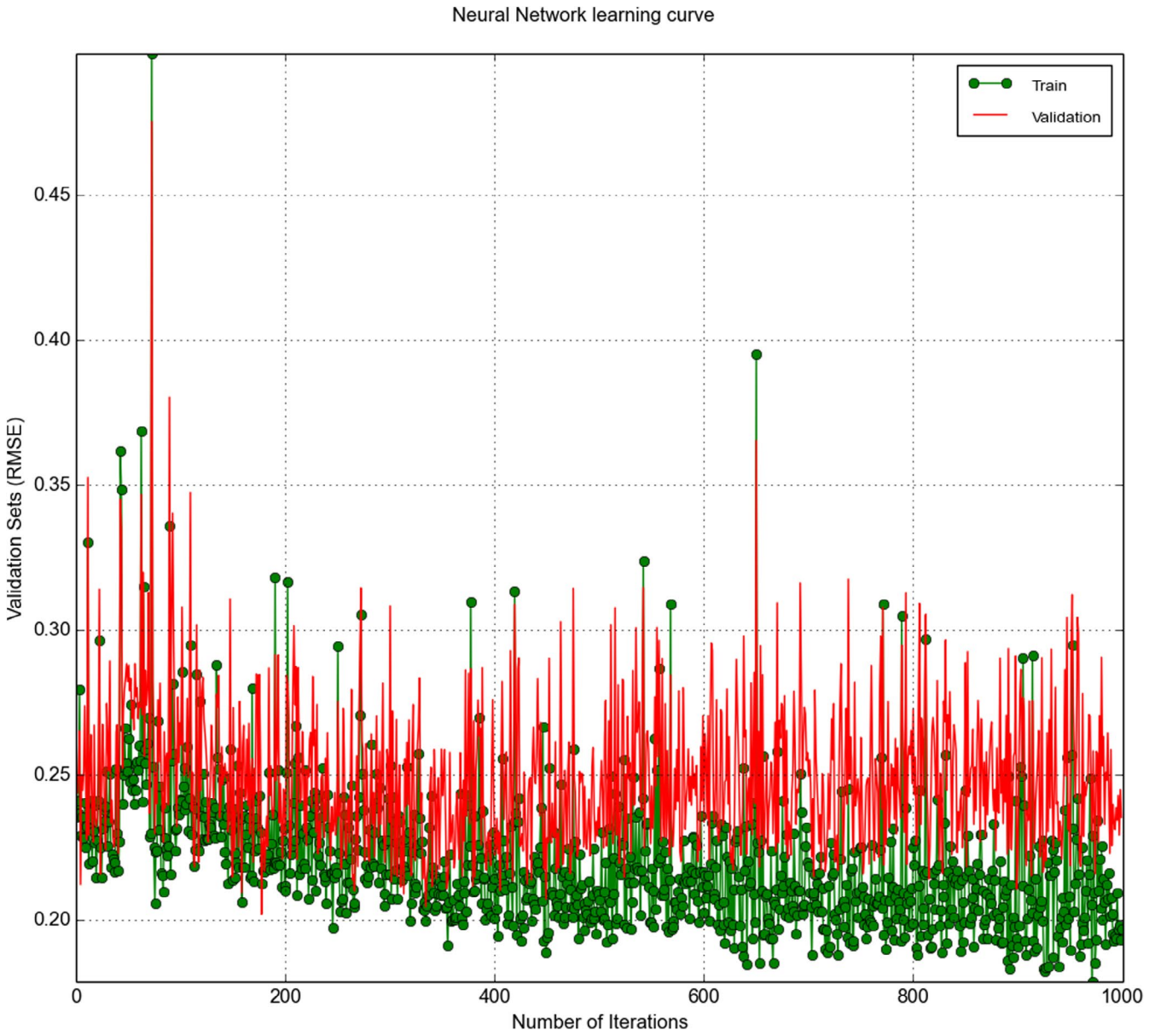

FIGURE 7 | Neural network learning curve.

concerns about habitat fragmentation and its cascading effects on wildlife. The reappearance of bare land in 2024 might suggest that the classification algorithm failed to consistently identify this land-cover type, possibly due to different atmospheric conditions, sensor resolutions, or classification thresholds (Abidi 2024; Cecili 2024). However, bare land might be temporarily converted for agriculture, explaining its disappearance in 2022, and partially abandoned or reverted to bare land in 2024. Moreover, bare land may experience some vegetation regrowth (e.g., shrubs or grasses) in 2022, making it appear less "bare," and subsequent land-use activities in 2024 could expose parts of it again. The strong decrease in forest suggests that deforestation could be exposing more bare land by 2024. If human or natural dynamics (e.g., deforestation or land abandonment) align with this pattern, the observed changes might reflect actual land-cover transitions rather than classification errors. Observations from the classified images show that the 2024 simulated map does not match the 2020, 2022, and 2024 maps. The 2024 map has a much smaller amount of forest than the 2024 simulated, and there are many differences in the bare lands. The simulated map in a cellular automata (CA) model is often different from the actual map for a given year because the simulated map is a product of the model's assumptions, rules, and parameters, while the actual map represents real-world conditions influenced by a wide range of unpredictable factors (Abidi 2024; Cecili 2024). Cellular automata models are simplified representations of complex systems. They rely on predefined transition rules, parameters, and assumptions (e.g., probabilities of change, neighbourhood effects, or constraints) that attempt to capture how land use or other factors evolve over time. The simplifications may miss finer details or complex interactions that occur in the real world. However, real-world changes do not always align perfectly with these steps. Some transitions might occur earlier or later than the model predicts. The simulated map for 2024 might reflect a change that actually occurred earlier or has not yet occurred in reality by 2024. Thus, differences between simulated and actual maps arise

because the CA model is a simplified representation of reality. These differences reflect the influence of external, unpredictable factors, modelling limitations, and data quality issues, but they also provide opportunities to refine the model and enhance its predictive power. The differences between the simulated and actual maps are not always a problem—they provide valuable information for improving the model.

On another note, the model predicts a scenario in 2028 compared to a simulated situation in 2024. The comparison between these two scenarios is plausible as demonstrated by the PCAF of residual analyses and also the Neural Network learning curve. But the key point is that the simulated map on which the model is built does not match the previously observed maps of 2020, 2022, and even 2024. The explanation for such a scenario is that the predicted map in a Cellular Automata (CA) model for 2028 is different from the actual maps for 2020, 2022, and 2024 due to the interplay between model assumptions, simplifications, data quality, and the inherent unpredictability of real-world systems. Cellular Automata models rely on simplified transition rules and assumptions about how changes (e.g., urban growth, deforestation) occur over time. These rules may not fully capture the complex, non-linear interactions of real-world processes. Assumptions often include uniform behaviour within specific land classes (e.g., all agricultural areas have the same probability of converting to urban land), which may not reflect localised variations. The predicted map may oversimplify or generalise patterns that are more complex in reality, resulting in differences when compared to observed maps. Real-world land-cover changes are influenced by external, unpredictable factors that the CA model cannot foresee, such as policy changes (e.g., environmental protections, urban development plans); economic shifts (e.g., recession or investment in infrastructure); natural disasters (e.g., floods, wildfires); and technological innovations (e.g., precision agriculture, renewable energy projects). These events can drastically alter the trajectory of land-use patterns but are not included in the model's scope. The predicted map does not account for these factors, leading to deviations from actual trends.

The fluctuations in forest, grassland, and bareland areas directly impact the availability and quality of habitats for wildlife in the Charara Safari Area. The reduction in grassland and the expansion of bareland, particularly in recent years, signal a loss of key habitats, leading to increased competition for resources among wildlife populations. Forest cover, which initially increased between 2020 and 2022, has since declined, further reducing critical habitats for species that rely on forested areas for protection and sustenance. Agricultural expansion into the park has exacerbated habitat fragmentation, creating more edge zones where human-wildlife interactions are frequent. These edge zones are hotspots for conflict, as wildlife often ventures into agricultural fields in search of food, making them vulnerable to retaliatory or opportunistic poaching. The decline in grassland and the fluctuating trends in bareland also indicate land degradation, which can reduce the carrying capacity of the ecosystem and force wildlife into closer proximity to human settlements. The intensification of wire snare poaching in the Charara Safari Area is closely linked to the observed LULC changes. Wire snares are inexpensive and widely used by local communities for subsistence hunting or as a response to human-wildlife conflict. Buffalo, impala, kudu, and warthog are particularly vulnerable due to their feeding and movement patterns, which often bring them into conflict with expanding agricultural areas. The temporal patterns of wire snare poaching align closely with the seasonal dynamics of agricultural activities and wildlife movements. During planting and harvesting seasons, wildlife is more likely to encroach on agricultural fields, leading to an increase in snaring activity. Similarly, during the dry season, when water sources become scarce, animals congregate in predictable locations, making them easier targets for poachers. The classified LULC data show that areas of high habitat fragmentation, particularly along the boundaries of forest and grassland, correspond to regions of intense poaching activity. The decline in grassland areas and the increase in bareland from 2022 to 2024 likely exacerbate this trend. As grasslands shrink, species like impala and warthog, which rely on these habitats for grazing, are forced into smaller, more fragmented patches. This increases their exposure to snares, especially in areas where agricultural fields encroach on natural habitats. Similarly, the decline in forest cover reduces shelter for species like kudu and buffalo, making them more susceptible to poaching. The intensity of wire snare poaching is influenced not only by habitat changes but also by socioeconomic factors. As agricultural expansion reduces the availability of natural resources, local communities face increased pressure to exploit wildlife for subsistence or income. The observed expansion of bareland and the corresponding loss of grassland and forested areas suggest a growing imbalance between human needs and ecological sustainability. The impact of poaching is particularly severe for species targeted by wire snares (Martin et al. 2020; Loveridge et al. 2020). These losses have cascading effects on the ecosystem, disrupting food webs and altering species interactions. For instance, the decline of herbivores like buffalo and impala can lead to overgrowth of certain plant species, while the loss of prey species like warthog can affect predator populations. The changes in LULC and the associated increase in poaching pressure have broader ecological implications for the Charara Safari Area. The loss of key species disrupts ecosystem functions such as herbivory, seed dispersal, and nutrient cycling. Furthermore, the shift in land use patterns may lead to long-term changes in wildlife behaviour. As habitats become increasingly fragmented, animals may alter their movement patterns, reducing genetic diversity and increasing vulnerability to environmental changes. This, in turn, affects the resilience of the ecosystem, making it less capable of adapting to future challenges such as climate change or further human encroachment.

To mitigate the impacts of LULC changes and poaching in the Charara Safari Area, an integrated approach is needed. Key recommendations include: Habitat Restoration: Efforts should focus on restoring degraded grasslands and reforesting bareland areas. This could involve planting native vegetation, controlling invasive species, and establishing wildlife corridors to enhance connectivity. Community Engagement: Engaging local communities is crucial for reducing poaching. Alternative livelihoods, such as sustainable agriculture, ecotourism, or employment in conservation projects, can help alleviate socioeconomic pressures driving poaching. Anti-Poaching Measures: Strengthening law enforcement and surveillance, including the use of drones and camera traps, can help deter poaching. Training and equipping rangers to monitor high-risk areas is also essential. Monitoring and Research: Continued monitoring of LULC changes using remote sensing and classified imagery is critical for tracking habitat trends and

predicting poaching hotspots. Research on wildlife movements and population dynamics can further inform conservation strategies. Policy and Planning: Implementing land-use policies that balance agricultural expansion with wildlife conservation is essential. Zoning regulations, buffer zones, and incentives for sustainable practices can help reduce habitat encroachment.

The classified images of LULC changes in the Charara Safari Area provide a clear picture of the challenges facing this ecosystem. Agricultural expansion and habitat fragmentation are driving changes that increase the vulnerability of wildlife to wire snare poaching. The temporal patterns and intensity of poaching are closely tied to these land use dynamics, highlighting the interconnectedness of ecological and socioeconomic factors. Addressing these challenges requires a holistic approach that combines habitat restoration, community engagement, anti-poaching efforts, and ongoing monitoring. By taking these steps, it is possible to preserve the biodiversity and ecological integrity of the Charara Safari Area while supporting the livelihoods of local communities. Projected LULC changes for 2028 inform conservation strategies by identifying potential threats to ecological integrity. For instance, declining forest cover may indicate increasing anthropogenic pressure, necessitating stricter protection measures. Grassland shifts could signal habitat loss for key wildlife species, while changes in water bodies affect ecosystem services. The model's reliability was further evaluated using a neural network learning curve, where decreasing training loss indicated improved prediction capabilities. By integrating satellite imagery, advanced classification techniques, and predictive modelling, this study enhances understanding of ecological trends in the Charara Safari Area. These insights support proactive conservation planning, ensuring sustainable land use while mitigating environmental degradation. The methodology demonstrates the power of remote sensing and machine learning in ecological monitoring, reinforcing their role in guiding data-driven conservation efforts.

Acknowledgements

The authors would like to acknowledge the role of anonymous reviewers who helped to enhance the quality of the work. Special thanks goes to the former Director General of Zimbabwe Parks and Management Authority, Dr. F.U. Mangwanya for giving us permission to conduct this research.

Conflicts of Interest

The authors declare no conflicts of interest.

Data Availability Statement

The data that support the findings of this study are available on request from the corresponding author. The data are not publicly available due to privacy or ethical restrictions.

References

Abidi, A. 2024. "Investigating Deep Learning and Image-Encoded Time Series Approaches for Multi-Scale Remote Sensing Analysis in the Context of Land Use/Land Cover Mapping." (Doctoral dissertation, Université de la Manouba (Tunisie); Université de Montpellier).

Banerjee, S., T. Kauranne, and M. Mikkila. 2020. "Land Use Change and Wildlife Conservation—Case Analysis of LULC Change of Pench-Satpuda Wildlife Corridor in Madhya Pradesh, India." *Sustainability* 12, no. 12: 4902.

Battisti, C. 2024. "Ecological Networks as Planning Tools for African Fragmented Landscapes: Overcoming Weaknesses for an Effective Connectivity Conservation." *African Journal of Ecology* 62, no. 1: e13186. https://doi.org/10.1111/aje.13186.

Becker, M. S., S. Creel, M. Sichande, et al. 2024. "Wire-Snare Bushmeat Poaching and the Large African Carnivore Guild: Impacts, Knowledge Gaps, and Field-Based Mitigation." *Biological Conservation* 289: 110376. https://doi.org/10.1016/j.biocon.2023.110376.

Cecili, G. 2024. "Classification of Land Cover in Urban and Periurban Regions Using Supervised Machine Learning Algorithms."

Chakuya, J., R. Mandisodza-Chikerema, P. Ngorima, and A. Malunga. 2023. "Water Sources During Drought Period in a Savanna Wildlife Ecosystem, Northern Zimbabwe." *Geology, Ecology, and Landscapes* 7, no. 4: 323–328.

Diebold, F. X., and G. D. Rudebusch. 2011. *The Dynamic Nelson-Siegel Approach to Yield Curve Modeling and Forecasting*. Princeton University Press.

Djagoun, C., and P. Gaubert. 2009. "Small Carnivorans From Southern Benin: A Preliminary Assessment of Diversity and Hunting Pressure." *Small Carnivore Conservation* 40: 1–10.

Dunham, K., C. Mackie, and G. Nyaguse. 2015. *Aerial Survey of Elephants and Other Large Herbivores in the Zambezi Valley (Zimbabwe): 2014. Great Elephant Census*, 118. Vulcan Inc.

Eniang, E. A., C. O. Ebin, A. A. Nchor, et al. 2017. "Distribution and Status of the African Forest Buffalo *Syncerus caffer Nanus* in South-Eastern Nigeria." *Oryx* 51, no. 3: 538–541.

Fentaw, T., and J. Duba. 2017. "Human–Wildlife Conflict Among the Pastoral Communities of Southern Rangelands of Ethiopia: The Case of Yabello Protected Area." *Journal of International Wildlife Law & Policy* 20, no. 2: 198–206.

Loveridge, A., L. Sousa, J. Seymour-Smith, et al. 2020. "Evaluating the Spatial Intensity and Demographic Impacts of Wire-Snare Bush-Meat Poaching on Large Carnivores." *Biological Conservation* 244: 108504.

Madden, F. 2004. "Creating Coexistence Between Humans and Wildlife: Global Perspectives on Local Efforts to Address Human–Wildlife Conflict." *Human Dimensions of Wildlife* 9, no. 4: 247–257.

Martin, E. A., G. R. Brull, S. M. Funk, L. Luiselli, R. Okale, and J. E. Fa. 2020. "Wild Meat Hunting and Use by Sedentarised Baka Pygmies in Southeastern Cameroon." *PeerJ* 8: e9906. https://doi.org/10.7717/peerj.9906.

Moore, J. F., F. Mulindahabi, M. K. Masozera, et al. 2018. "Are Ranger Patrols Effective in Reducing Poaching-Related Threats Within Protected Areas?" *Journal of Applied Ecology* 55, no. 1: 99–107.

Mukomberanwa, N. T., P. Taru, B. Utete, and H. K. Madamombe. 2024. "Predicting the Dry Season Habitat Occupancy of African Savannah Elephant Using Vegetation Indices and Modelling Landscape Variability in a Mesic Protected Area." *African Journal of Ecology* 62, no. 3: e13318. https://doi.org/10.1111/aje.13318.

R Development Core Team. 2022. *R: A Language and Environment for Statistical Computing*. R Foundation for Statistical Computing.

Wato, Y. A., G. M. Wahungu, and M. M. Okello. 2006. "Correlates of Wildlife Snaring Patterns in Tsavo West National Park, Kenya." *Biological Conservation* 132, no. 4: 500–509. https://doi.org/10.1016/j.biocon.2006.05.010.

Watson, F., M. S. Becker, R. McRobb, and B. Kanyembo. 2013. "Spatial Patterns of Wire-Snare Poaching: Implications for Community Conservation in Buffer Zones Around National Parks." *Biological Conservation* 168: 1–9.

Appendix 1

Land use and land cover for the years 2020, 2022, and 2024 used for land change modelling.

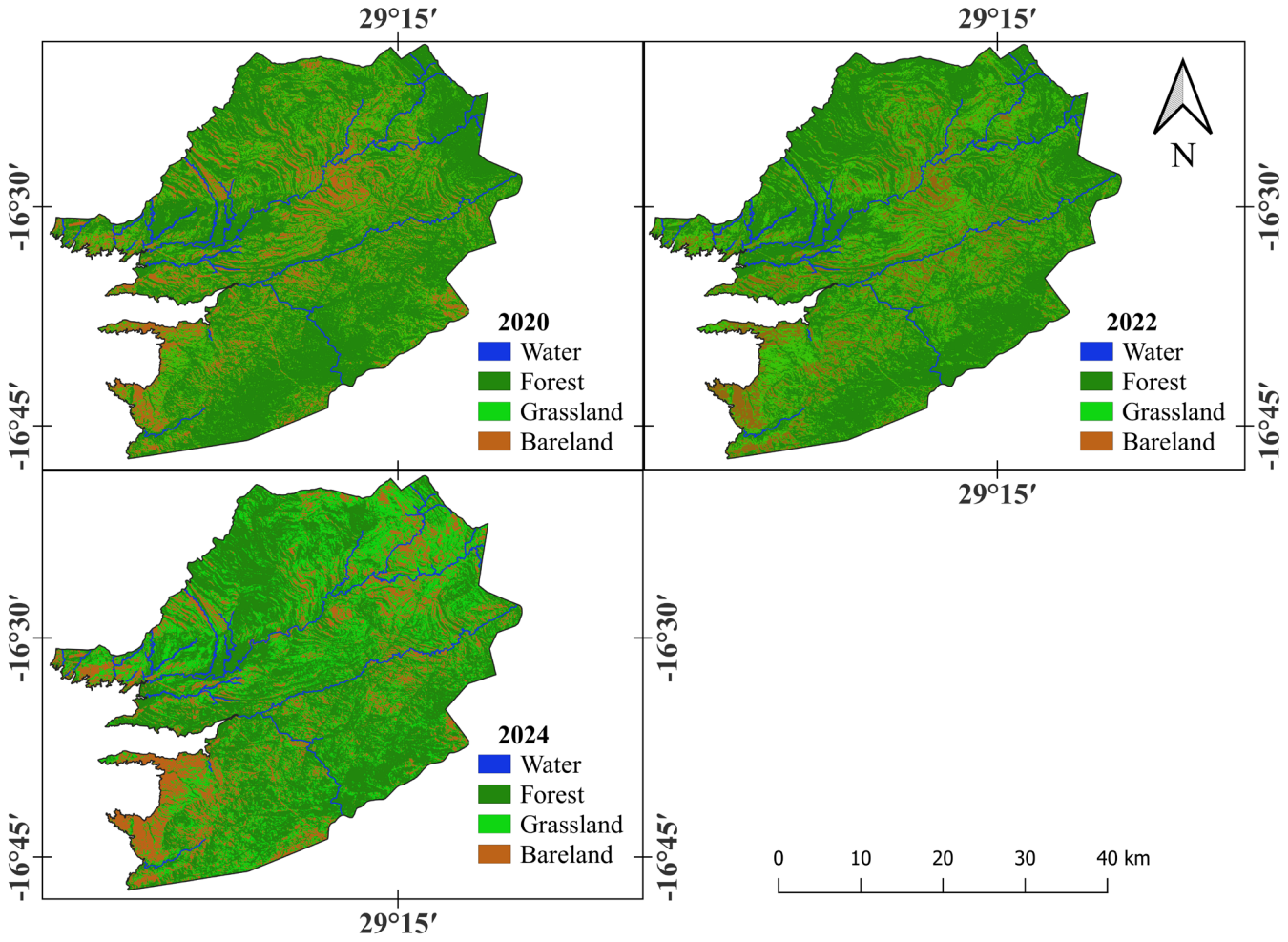

Appendix 2

Spatial variables used as inputs in land change modelling, Digital Elevation Model (DEM) and slope of Charara Safari Area.

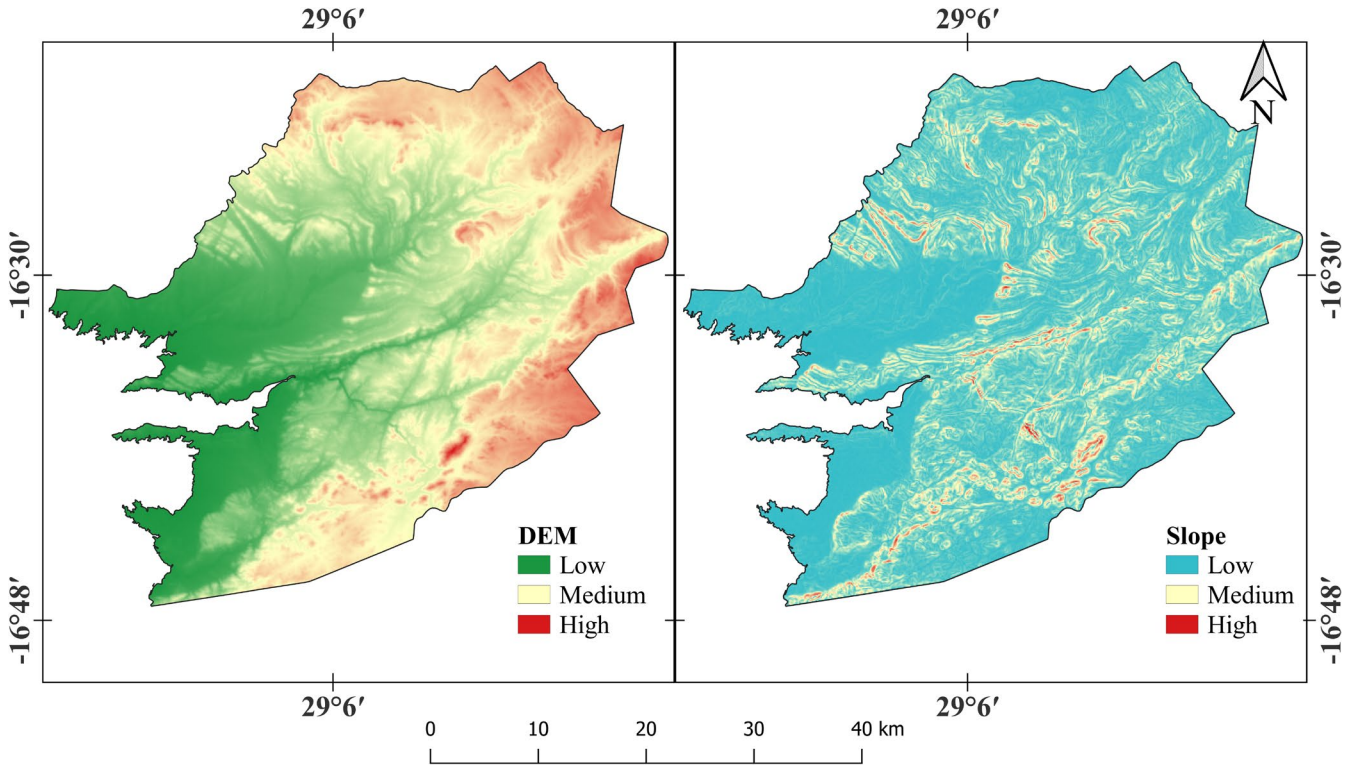

Appendix 3

Change Map (2020–2022). The change map identifies regions in the cellular grid where state transitions (e.g., land use change, urban growth) occur. Patterns reveal the spatial behaviour of the system and the dynamics driving changes.

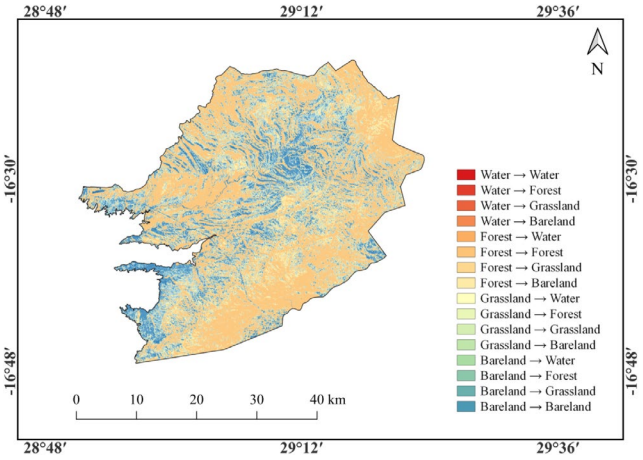

Appendix 4

Multiple resolution budget. High-resolution regions indicate areas of interest or high activity, while low-resolution regions suggest areas of stability or less importance. Dynamic adjustments in resolution indicate that the model is responsive to system changes, enhancing its ability to represent real-world dynamics.